frontiers | Frontiers in Marine Science

TYPE Original Research
PUBLISHED 11 November 2022
DOI 10.3389/fmars.2022.1050022

OPEN ACCESS

EDITED BY
Taewoo Ryu,
Okinawa Institute of Science and Technology Graduate University, Japan

REVIEWED BY
Liqiang Zhao,
Guangdong Ocean University, China
Yuehuan Zhang,
South China Sea Institute of Oceanology (CAS), China

*CORRESPONDENCE
Chang Liu
liuchang@dlou.edu.cn
Linsheng Song
lshsong@dlou.edu.cn

SPECIALTY SECTION
This article was submitted to Marine Molecular Biology and Ecology, a section of the journal Frontiers in Marine Science

RECEIVED 21 September 2022
ACCEPTED 26 October 2022
PUBLISHED 11 November 2022

CITATION
Xin X, Liu C, Liu Z, Zhang Y, Gao Y, Zhu T, Wang L and Song L (2022) Calmodulin regulates the calcium homeostasis in mantle of *Crassostrea gigas* under ocean acidification. *Front. Mar. Sci.* 9:1050022. doi: 10.3389/fmars.2022.1050022

Calmodulin regulates the calcium homeostasis in mantle of *Crassostrea gigas* under ocean acidification

Xiaoyu Xin[1,2,3], Chang Liu[1,2,3]*, Zhaoqun Liu[1,2,3], Yukun Zhang[1,2,3], Yuqian Gao[1,2,3], Ting Zhu[1,2,3], Lingling Wang[1,2,3,4] and Linsheng Song[1,2,3,4]*

[1]Liaoning Key Laboratory of Marine Animal Immunology, Dalian Ocean University, Dalian, China, [2]Liaoning Key Laboratory of Marine Animal Immunology and Disease Control, Dalian Ocean University, Dalian, China, [3]Dalian Key Laboratory of Aquatic Animal Disease Prevention and Control, Dalian Ocean University, Dalian, China, [4]Functional Laboratory of Marine Fisheries Science and Food Production Processes, Qingdao National Laboratory for Marine Science and Technology, Qingdao, China

The biosynthesis of shell is a complicated calcification process in the marine bivalve, which can be severely impacted by ocean acidification (OA). Calmodulin (CaM) is a pivotal calcium regulator and thought to be crucial for calcification. In the present study, a CaM (designated *Cg*CaM) with calcium-binding activity was identified from the Pacific oyster *Crassostrea gigas* with the objective to understand its possible role in the regulation of calcium homeostasis under acidification treatment. The open reading frame (ORF) of *Cg*CaM was of 474 bp encoding a 17.5 kDa protein with four continuous EF-hand domains. *Cg*CaM shared high similarity with CaMs from other invertebrates and vertebrates. The mRNA transcript of *Cg*CaM was constitutively expressed in all detected tissues with the higher expression level in mantle, especially highest in the middle fold of the three folds of mantle. *Cg*CaM was found to be mainly distributed in the mantle epithelium. When the oysters were exposed to acidified seawater, the expression level of *Cg*CaM in the middle fold of mantle and the content of Ca^{2+} in this fold both decreased significantly. These results collectively suggested that *Cg*CaM was involved in the regulation of calcium homeostasis in the middle fold of mantle under acidification treatment.

KEYWORDS

ocean acidification, calmodulin, calcium homeostasis, mantle, *Crassostrea gigas*

Introduction

Bivalves are a large taxon of calcifying organisms in the ocean, and they have developed tough shell through biologically controlled mineralization process to protect them against predation, support tissues and preclude desiccation (Simkiss and Wilbur, 1989; Marin et al., 2012). The bivalve shell is a typical calcium carbonate ($CaCO_3$) biomineral consisting of approximately 95% $CaCO_3$ and a low proportion of organic matrix, with aragonite and calcite as the main crystalline polymorphs (Marin et al., 2008). In recent years, increasing amounts of atmospheric CO_2 was absorbed by the ocean, and the pH value of the seawater was decreased (Caldeira and Wickett, 2003), which called ocean acidification (OA). According to the previous prediction, the pH of the ocean surface is projected to reduce from 8.10 to 7.80 by the end of 2100. Many evidences have demonstrated that ocean acidification (OA) alters the chemical equilibrium of seawater and hence affects the ion homeostasis such as calcium homeostasis in marine bivalves (Li et al., 2016a; Li et al., 2016b), which results in limitation of their growth, development and reproduction (Ross et al., 2011; Hettinger et al., 2013), and even death (Waldbusser et al., 2013).

OA has been demonstrated to disrupt the calcification process of bivalves by affecting the homeostasis of calcium levels (Bednaršek et al., 2014; Chandra Rajan et al., 2021), and the driving mechanism of calcium homeostasis is crucial for bivalves in response to OA. The calcification rate of marine bivalves is reduced due to the decrease of $CaCO_3$ saturation in seawater under elevated CO_2 levels (Richards et al., 2018; Chandra Rajan and Vengatesen, 2020). As the main component of shell, sufficient calcium is required for shell calcification. The calcium needed for calcification is mainly absorbed from the external medium in the form of calcium ion (Ca^{2+}) *via* gill and mantle, then transported to the mineralization sites across mantle by hemocytes (Mount et al., 2004; Addadi et al., 2006; Marin et al., 2012). As the main organ of bivalves for calcification, mantle positively participates in calcium regulation (Li et al., 2004; Sillanpää et al., 2020; Wang et al., 2022). Mantle is composed of inner muscles, nerve fibers and connective tissues bordered by epithelium cell layers on either side (Audino et al., 2015). According to the functional heterogeneity and morphological difference, the mantle is separated into marginal, submarginal and central zone (Fang et al., 2008a). The marginal zone of the mantle has been demonstrated to be particularly active in calcification, and it is further divided into outer fold (OF), middle fold (MF) and inner fold (IF) (Kádár, 2008). The molecular mechanism involved in calcium regulation of mantle is critical to comprehensively understand the adaptation of marine bivalves to OA.

Calmodulin (CaM) is a well-studied calcium-binding protein with EF-hand domains that are widely distributed in all eukaryotic cells (Stevens, 1983). Upon binding to Ca^{2+}, CaM undergoes activity changes and subsequently interacts with downstream proteins to mediate a variety of Ca^{2+}-induced physiological processes (Clapham, 2007), such as cell proliferation, differentiation, apoptosis, glycogen metabolism, and calcium metabolism (Means and Dedman, 1980; Cheung, 1984; Sée et al., 2001). As a fast Ca^{2+} buffer and pivotal Ca^{2+} sensor, CaM plays an important role in calcium metabolism processes including calcium absorption, transportation, secretion and deposition (Schwaller, 2012). In vertebrates, the calcium homeostasis is modulated by CaM, which activates or inactivates functional enzymes, cellular receptors and ion channels involved in Ca^{2+} transportation to affect intracellular Ca^{2+} concentration (Zhou et al., 2013). In *Stylophora pistillata*, the interaction of CaM and plasma-membrane Ca^{2+}-ATPase was reported to regulate calcareous skeleton deposition (Zoccola et al., 2004). Several CaMs have been characterized to participate in calcification in bivalves. The CaM in *Hyriopsis schlegelii* was found to be highly expressed in pearl sac and promote the pearl sac formation (Peng et al., 2018). In the Pacific oyster *Crassostrea gigas*, the intracellular calcium levels varied significantly after a short-term (7 days) CO_2 exposure. While the long-term (60 days) CO_2 exposure activated the CaM related signal pathway, and the intracellular calcium recovered to normal levels (Wang et al., 2020). Accumulating reports suggest that CaM is of vital importance in the regulation of bivalve calcium homeostasis under acidification treatment. However, the exact regulatory mechanisms are still not well understood.

The Pacific oyster *C. gigas* is an important marine calcifying species and a worldwide aquaculture species with economic and ecological significance to the ecosystem (Hendriks et al., 2015). They are distributed in coastal areas worldwide with calcified shells to protect themselves from diverse environmental fluctuations. In the present study, a novel calmodulin (designated *Cg*CaM) was characterized from *C. gigas* with the main objectives to (1) investigate its expression and distribution in tissues, (2) determine its calcium-binding activity *in vitro*, and (3) examine the alteration of its expression and calcium content in the MF of mantle after acidification treatment to understand its possible role in the regulation of calcium homeostasis under OA.

Materials and methods

Oyster, acidification treatment and sample collection

The adult Pacific oysters (*C. gigas*) with an average shell length of 15.0 cm were obtained from a local breeding farm in Dalian, Liaoning province, China. The oysters were pre-acclimated in normal aerated seawater for one week before processing. The experiments were approved by the animal

ethics guidelines approved by the Ethics Committee of Dalian Ocean University.

Twenty-four oysters were randomly divided into two groups. The oysters cultured in normal aerated seawater were designated as the control group (pH 8.10 ± 0.05), while those cultured in the seawater continuously bubbled with the air-CO_2 mixtures were designated as CO_2 treatment group (pH 7.80 ± 0.05). The pH value was controlled using an acidometer (AiKB, China) according to previous reports (Zhang et al., 2019). The partial pressure of CO_2 was about 658.1 ± 11.0 ppm and 1217.3 ± 11.6 ppm in pH 8.10 and pH 7.80 groups. And total alkalinity was determined by end-point titration of 25 mmol/L HCl on 50 mL seawater samples.

Oyster samples were collected from each group on 14th day after acidification treatment. Mantle, gill, adductor muscle, hepatopancreas, hemolymph and labial palp were collected from twelve oysters in the control group and CO_2 treatment group respectively. The samples from four individuals were randomly mixed as one replicate, and there were three replicates for each group. The hemolymph was extracted and immediately centrifuged at 800 × *g*, 4°C for 15 min to harvest the hemocytes. The mantle was separated into IF, MF and OF under the microscope Discovery V8 (ZEISS, Germany). The samples for RNA extraction were kept in 1 mL TRIzol reagent (Invitrogen, USA) and stored at -80°C, while the samples for *in situ* hybridization were fixed with fixative solution (Servicebio, China) for further processing.

Total RNA extraction and cDNA synthesis

Total mRNA was extracted from tissues with TRIzol reagent (Invitrogen, USA) according to the manual. The synthesis of the first-strand cDNA was carried out based on M-MLV RT Usage information (Promega, USA) using the total mRNA treated with DNase I (Takara, China) as template and oligo (dT)-adaptor as primer. The synthesis reaction was first incubated at 42°C for 1 h, and then terminated by heating at 95°C for 5 min. The cDNA mix was diluted and stored at -80°C for subsequent quantitative real-time PCR.

Gene cloning and sequence analysis

According to the sequence information from the National Center for Biotechnology Information (http://www.ncbi.nlm.nih.gov/), the open reading frame (ORF) of *Cg*CaM (XM_011428724) was amplified using the specific primers *Cg*CaM-F and *Cg*CaM-R (Table 1). The PCR product was cloned into pMD19-T simple vector (Takara, China) and confirmed by DNA sequencing.

The deduced amino acid sequence was analyzed with the Expert Protein Analysis System (http://www.expasy.org/). The homology searches of the cDNA sequences and protein sequences were conducted with BLAST algorithm (http://www.ncbi.nlm.nih.gov/blast). The protein domain and signal peptide were predicted with the Simple Modular Architecture Research Tool (SMART, http://www.smart.emblheidelberg.de/). ClustalW multiple alignment program was used to create the multiple sequence alignment (http://www.ebi.ac.uk/Tools/clustalw2/). The phylogenetic tree was constructed with the Mega 7.0 program.

Quantitative real-time PCR analysis

The *Cg*CaM mRNA expression level in different tissues was measured by SYBR Green fluorescent quantitative real-time PCR (qRT-PCR) in an ABI PRISM 7500 Sequence Detection System. Specific primers *Cg*CaM-RT-F and *Cg*CaM-RT-R (Table 1) were used to amplify the fragment of *Cg*CaM. The *C. gigas* elongation factor (*Cg*EF) fragment amplified with primers *Cg*EF- F and *Cg*EF-R (Table 1) was used as internal control. The qRT-PCR experiment was conducted according to previous description (Lv et al., 2019). The relative expression of genes was determined by $2^{-\Delta\Delta Ct}$ method (Livak and Schmittgen, 2001).

In situ hybridization

The mantle tissues were embedded in paraffin and cut into 5 μm thick sections according to previous report (Johnson et al., 2000; Zhang et al., 2020). *In situ* hybridization of *Cg*CaM mRNA was carried out on these sections. Digoxigenin-labeled RNA probes were synthesized using a DIG RNA Labeling Kit (Roche, Germany) and detected by a DIG Nucleic Acid Detection Kit (Roche, Germany). The detailed step was performed following the previous reports (Johnson et al., 2000; Huang et al., 2001).

TABLE 1 Sequences of the primers used in this study.

Primer	Sequence (5'-3')
Clone primers	
*Cg*CaM-F	ATGGCACAGAGAGAGCAAATC
*Cg*CaM-R	GCCGTCCTTTTTACCAGA
Expression primers	
*Cg*CaM-Fe	CGCGGATCCATGGCACAGAGAGAGCAAATC
*Cg*CaM-Re	CCCAAGCTTGGCCGTCCTTTTTACCAGA
RT-PCR primers	
*Cg*CaM-RT-F	GAGAGCATTCGTGGCTTAGTTGT
*Cg*CaM-RT-R	AGTTCGCCCTCAGTGGGATTC
*Cg*EF- F	AGTCACCAAGGCTGCACAGAAAG
*Cg*EF- R	TCCGACGTATTTCTTTGCGATGT

Recombinant expression and purification

The recombinant protein of *Cg*CaM (r*Cg*CaM) was produced with the prokaryotic expression system. The coding region of *Cg*CaM was amplified using primers *Cg*CaM-Fe and *Cg*CaM-Re (Table 1) with *Bam*H I and *Hind* III enzyme cutting sites at their 5' end, respectively. The PCR products were digested with restriction enzymes *Bam*H I and *Hind* III, and ligated into predigested expression vector pET-30a (Novagen, Germany). The recombinant expression plasmid pET-30a-*Cg*CaM was transformed into *Escherichia coli* transetta (DE3) (TransGen, China) and the positive colony was incubated in LB medium at 37°C, 220 rpm. When the OD_{600} of culture medium reached 0.4-0.6, isopropyl-β-D-thiogalactopyranoside (IPTG) was added into the LB medium at the final concentration of 1 mM to induce the expression of r*Cg*CaM. Subsequently, r*Cg*CaM was purified by His-tag Purification Resin (Beyotime, China). Protein concentration was determined by BCA method and stored at -80°C for further experiments.

Ca^{2+} dependent electrophoretic migration

The electrophoretic migration assay was performed according to the previous method (Burgess et al., 1980; Senawong et al., 2012). The purified r*Cg*CaM protein was separated by 12% nondenaturing polyacrylamide gel electrophoresis in the presence of 20 mM ethylenediaminetetraacetic acid (EDTA) with 1 mM $MgCl_2$, or 1 mM $CaCl_2$, or without $MgCl_2$ and $CaCl_2$, respectively. Bovin serum albumin (BSA) was used as a control. The electrophoretic migration was observed by AI600 RGB.

Determination of intracellular Ca^{2+} levels

The mantle tissues harvested from *C. gigas* were minced and incubated with Pronase (2 mg mL^{-1}) in Hank's Balanced Salt Solution (HBSS) (G-CLONE, China) without Ca^{2+} or Mg^{2+} with a gentle shaking at 37°C for 4 h. The digested tissues were filtered (50 μm mesh), washed and centrifuged at 500 × *g* in HBSS for 10 min. The pellets were suspended in HBSS and the cell concentration was adjusted to 10^6 mL^{-1}. The mantle cells were incubated with Fluo-4 AM (5 μM) at 25°C in dark for 20 min. The median fluorescence intensity of 5000 cells was detected by FACS ImageStream^x Mark II and recorded as relative Ca^{2+} content (Föller et al., 2010).

Statistical analysis

All data were presented as mean ± S.D. and analyzed by Statistical Package for Social Sciences (SPSS) 16.0. Significant differences between samples were tested by one-way analysis of variance (ANOVA). The differences were considered as significant at $p < 0.05$.

Results

Sequence characteristics and phylogeny of *Cg*CaM

The complete ORF of *Cg*CaM was of 474 bp, encoding a polypeptide of 158 amino acids with a predicted molecular mass of 17.5 kDa and a theoretical isoelectric point of 4.22 (Figure 1A). There were four continuous typical EF-hand domains in *Cg*CaM (Figure 1B). The deduced amino acid sequence of *Cg*CaM shared high identity with those CaMs in other species (Figure 1C), such as 96.82%, 76.43%, 71.95%, 74.52%, 75.80%, 73.25%, 57.21% and 73.25% identity with that of *Crassostrea virginica*, *Pinctada fucata*, *Penaeus vannamei*, *Danio rerio*, *Drosophila melanogaster*, *Gallus gallus*, *Mus musculus* and *Homo sapiens*, respectively.

A phylogenetic tree was constructed to analyze the evolutionary relationship of *Cg*CaM with CaMs from other species by neighbor-joining method (Figure 1D). The *Cg*CaM was firstly clustered with calmodulin-A-like protein of *C. virginica* and then joined into the invertebrate group.

The mRNA expression of *Cg*CaM in different tissues

The mRNA transcripts of *Cg*CaM were detected in all the tested tissues, including hemocytes, hepatopancreas, adductor muscle, labial palp, gill and mantle with the highest expression level in mantle, which was 50.67-fold ($p < 0.05$) of that in hemocytes (Figure 2). *Cg*CaM was also highly expressed in gill and labial palp, which was 36.55-fold ($p < 0.05$) and 21.94-fold ($p < 0.05$) of that in hemocytes, respectively. There was no significant difference of *Cg*CaM mRNA expression among hemocytes, hepatopancreas and adductor muscle.

The mRNA expression of *Cg*CaM in different mantle folds under acidification treatment

The expression level of *Cg*CaM mRNA in IF, MF, OF and the whole mantle of oysters under acidification treatment were determined by quantitative real-time PCR analysis (Figure 3). In the control group, the highest expression level was detected in MF, which was 27.83-fold ($p < 0.05$) of that in IF. While the mRNA expression of *Cg*CaM in OF and the whole mantle were 11.03-fold ($p < 0.05$) and 7.75-fold ($p < 0.05$) of that in IF,

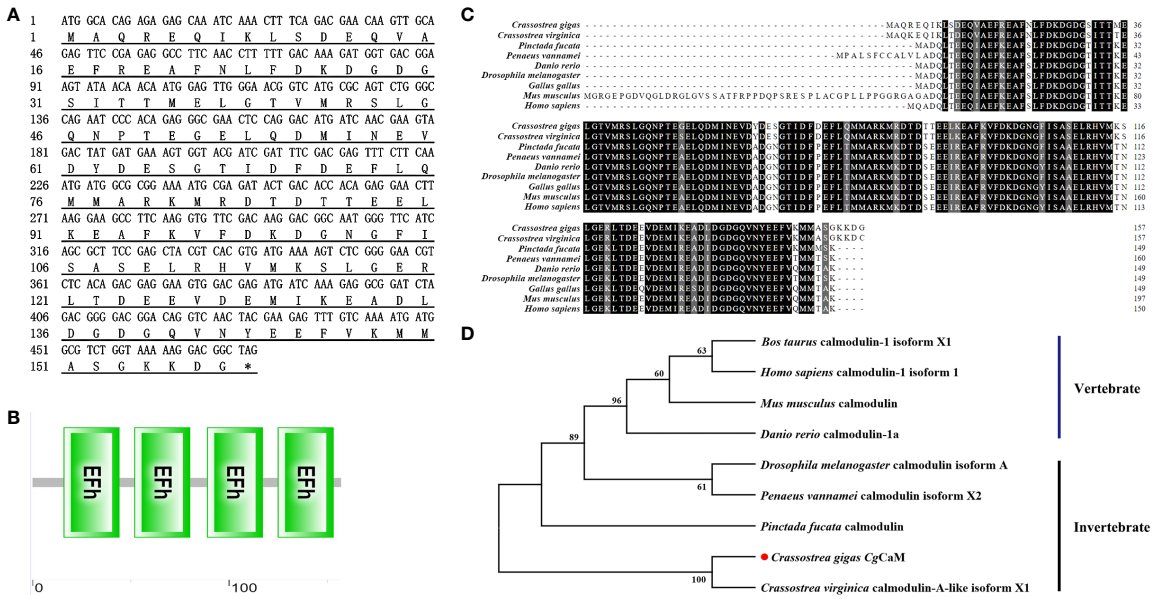

FIGURE 1
Bioinformatics analysis of *Cg*CaM. **(A)** Nucleotide and deduced amino acid sequence of *Cg*CaM. **(B)** Protein domains of *Cg*CaM predicted by SMART analysis. **(C)** Multiple sequence alignment of *Cg*CaM with known calmodulins from other species, including *Crassostrea virginica* (XP_022332301.1), *Pinctada fucata* (AAQ20043.1), *Penaeus vannamei* (ROT84624.1), *Danio rerio* (NP_892012.1), *Drosophila melanogaster* (NP_523710.1), *Gallus gallus* (NP_990336.1), *Mus musculus* (NP_001300863.1), *Homo sapiens* (NP_001350599.1). **(D)** Phylogenetic relationship of *Cg*CaM. Calmodulin sequences from different species were obtained from GenBank on NCBI, including *Bos taurus* calmodulin-1 isoform X1 (XP_024853610.1), *Homo sapiens* calmodulin-1 isoform 1 (NP_001350599.1), *Mus musculus* calmodulin (AAA66182.1), *Danio rerio* calmodulin-1a (NP_998516.1), *Drosophila melanogaster* calmodulin isoform A (NP_523710.1), *Penaeus vannamei* calmodulin isoform X2 (XP_027237663.1), *Pinctada fucata* calmodulin (AAQ20043.1), *Crassostrea gigas* CaM (XP_011427026.1), *Crassostrea virginica* calmodulin-A-like isoform X1 (XP_022332301.1).

respectively. After the acidification treatment for fourteen days, the mRNA expression level of *Cg*CaM in CO_2 treatment group was significantly down-regulated in MF, which was 0.13-fold ($p < 0.05$) of that in the control group. However, the mRNA expression level of *Cg*CaM in OF was up-regulated in CO_2 treatment group, which was 1.42-fold ($p < 0.05$) of that in the control group. There was no significant difference of *Cg*CaM mRNA expression in IF and the whole mantle under acidification treatment.

The distribution of *Cg*CaM mRNA transcripts in mantle under acidification treatment

The precise location of *Cg*CaM mRNA in the mantle tissue was analyzed *via in situ* hybridization. The positive hybridization signals of *Cg*CaM were observed in epithelium of the three mantle folds in the control group (Figure 4B). After acidification treatment, the positive signals in mantle epithelium were weakened, and no obvious positive signals were observed in the outer epithelium of MF (Figure 4D). No signals were detected in negative control group (Figures 4A, C).

Recombinant expression and calcium-binding activity of r*Cg*CaM

After IPTG induction, r*Cg*CaM was purified and analyzed by 12% SDS-PAGE. A distinct band was observed with a molecular mass about 25 kDa, which was consistent with the predicted molecular mass of r*Cg*CaM (Figure 5A).

To further confirm the calcium-binding activity of *Cg*CaM, Ca^{2+} dependent electrophoretic migration assay was performed. The purified r*Cg*CaM protein with the sample buffer were separated by PAGE (Figure 5B). After addition with 1 mM $CaCl_2$, the band of r*Cg*CaM was observed with obviously retardation effect. No mobility shift was observed in the presence of 1 mM $MgCl_2$. This result suggested that *Cg*CaM protein had calcium-binding activity.

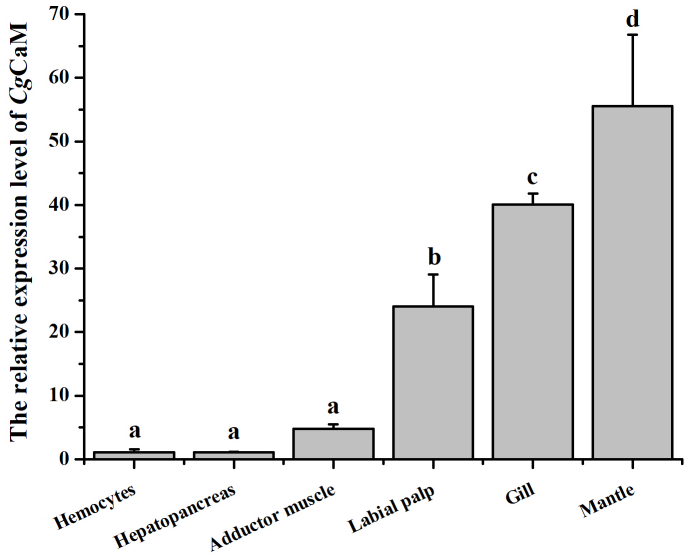

FIGURE 2
The mRNA expression level of *Cg*CaM in different tissues. Each value was shown as mean ± S.D. (N = 3), and the significant differences (p < 0.05) were marked by different letters (a-d).

Relative Ca^{2+} content in different folds of mantle under acidification treatment

The relative intracellular Ca^{2+} content in mantle cells of both control group and CO_2 treatment group were determined by flow cytometry (Figures 6B, C). In the control group, the Ca^{2+} content in IF and MF were significantly higher than that in OF, which were both 1.46-fold (p < 0.05) of that in OF. After acidification treatment, the relative intracellular Ca^{2+} content in CO_2 treatment group was significantly increased in IF, which

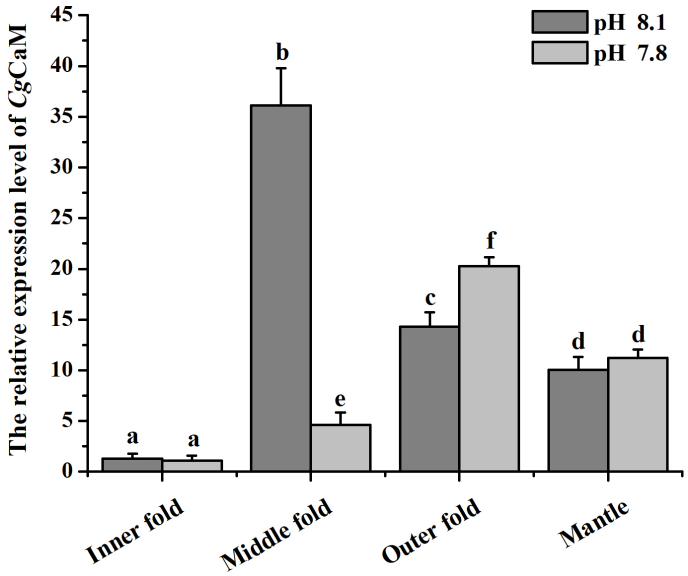

FIGURE 3
The mRNA expression level of *Cg*CaM in different folds of mantle under acidification treatment. Each value was shown as mean ± S.D. (N = 3), and the significant differences (p < 0.05) were marked by different letters (a-f).

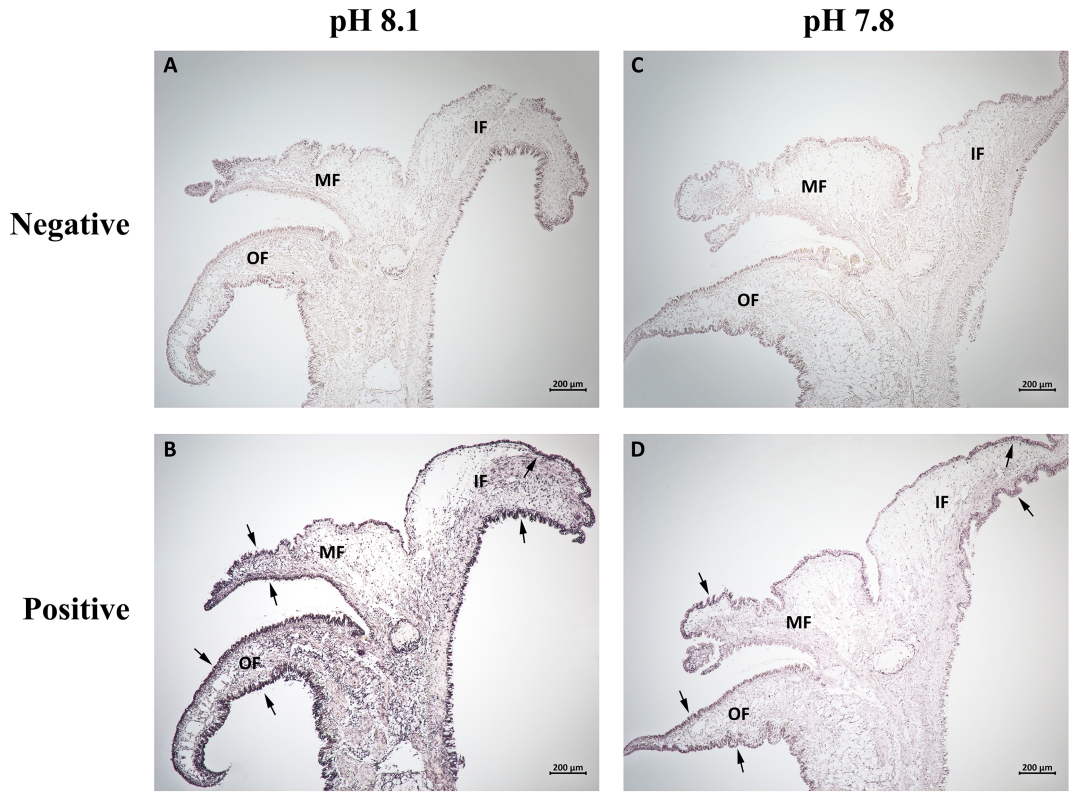

FIGURE 4
In situ hybridization analysis of *Cg*CaM mRNA in the mantle of oyster *C. gigas* under acidification treatment. The sections of the oyster mantle were **(A, C)** hybridized with the sense RNA probes as negative control, while **(B, D)** hybridized with the anti-sense RNA probes were the positive group. The hybridization positive signals were labeled with arrows. OF, outer fold; MF, middle fold; IF, inner fold.

was 1.23-fold ($p < 0.05$) of that in the control group. While the relative intracellular Ca^{2+} content in MF and the whole mantle were decreased in CO_2 treatment group, which was 0.62-fold ($p < 0.05$) and 0.81-fold ($p < 0.05$) of that in the control group, respectively. The results indicated that the Ca^{2+} content in IF, MF and the whole mantle all changed significantly after acidification treatment. It increased in IF but decreased in MF and whole mantle with showed the most dramatic drop in MF. No significant change of Ca^{2+} content in OF was observed after the treatment with CO_2 (Figure 6A).

Discussion

Due to the human activities, the emissions of CO_2 into the atmosphere is increasing (Field and Barros, 2014), and OA is becoming an irreversible environmental problem with further impacts on marine organisms (Feely et al., 2004; Orr et al., 2005). The calcified shells of bivalves play a vital protective role against environmental stresses, and the reduction of available carbonate saturation in seawater under OA may lead to difficulties in shell biosynthesis (Doney et al., 2009; Thomsen et al., 2015). The shell biosynthesis is a complicated calcification process, calcium homeostasis is crucial for bivalve calcification. CaM is proved to be a pivotal calcium regulator as well as shell formation participant in bivalves (Huang et al., 2007). In the present study, a CaM (designated *Cg*CaM) was identified from *C. gigas*, and its response against acidification was investigated to explore its possible role in regulation of calcium homeostasis within mantle under OA.

CaM is an important calcium-binding protein with typical EF-hand conformation (Babu et al., 1988). *Cg*CaM identified in the present study contained four continuous typical EF-hand domains (Figures 1A, B) located from 16 to 44 amino acids, 52 to 80 amino acids, 89 to 117 amino acids, and 125 to 153 amino acids. EF-hand is one of the most common calcium-binding domains in both vertebrates and invertebrates, which consists of a loop of twelve residues, and the six residues involved in Ca^{2+} binding are in positions 1, 3, 5, 7, 9 and 12 (Ikura, 1996; Kretsinger, 1997). As each EF-hand domain is able to bind one Ca^{2+}, the presence of four EF-hand domains in *Cg*CaM enables the mature *Cg*CaM protein to bind four calcium ions. The amino acid sequence of *Cg*CaM was found to share high homology with CaM from other invertebrates and vertebrates

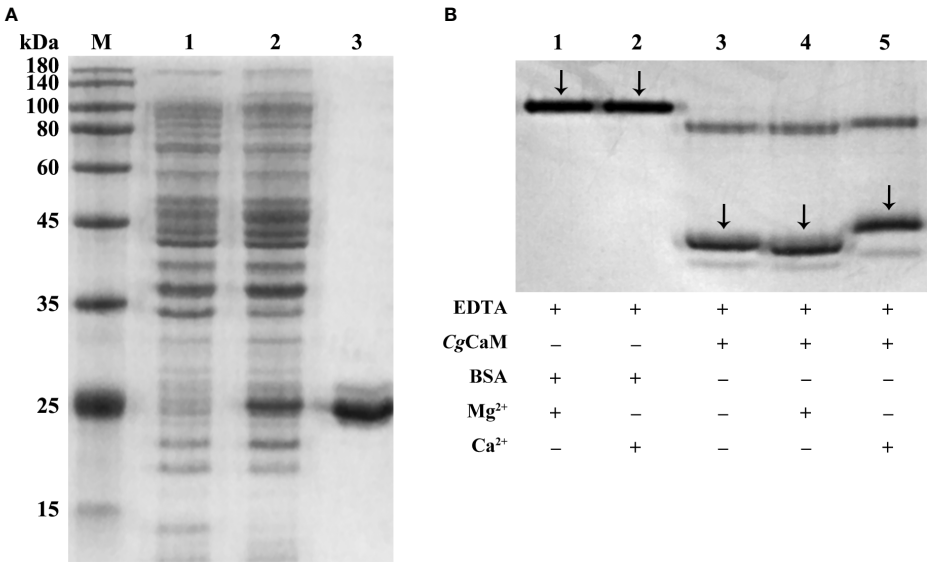

FIGURE 5
(A) SDS-PAGE analysis of r*Cg*CaM. Lane M: protein molecular standard (kDa); Lane 1: negative control without IPTG induction; Lane 2: positive transformant induced by IPTG; Lane 3: purified r*Cg*CaM. **(B)** Ca^{2+}-dependent electrophoretic migration analysis of purified r*Cg*CaM. Lane 1: BSA + 20 mM EDTA + 1 mM Mg^{2+}; Lane 2: BSA + 20 mM EDTA + 1 mM Ca^{2+}; Lane 3: r*Cg*CaM + 20 mM EDTA; Lane 4: r*Cg*CaM + 20 mM EDTA + 1 mM Mg^{2+}; Lane 5: r*Cg*CaM + 20 mM EDTA + 1 mM Ca^{2+}.

(Figure 1C). In the phylogenic tree, *Cg*CaM was clustered with CaM from other bivalves such as *C. virginica* and *P. fucata* (Figure 1D). These results suggested that *Cg*CaM belonged to the calcium-binding protein family, which might exhibit the similar functions as its homologues in other invertebrates and vertebrates.

It has been reported that CaM plays an important role in calcification process of marine bivalves. A calmodulin-like protein (CaLP) from pearl oyster *P. fucata* was reported to modify shell calcite morphology, and the aragonite crystals could be induced when a nacre protein was mixed CaLP (Yan et al., 2007). A mutant of CaLP distributed in mantle epithelium

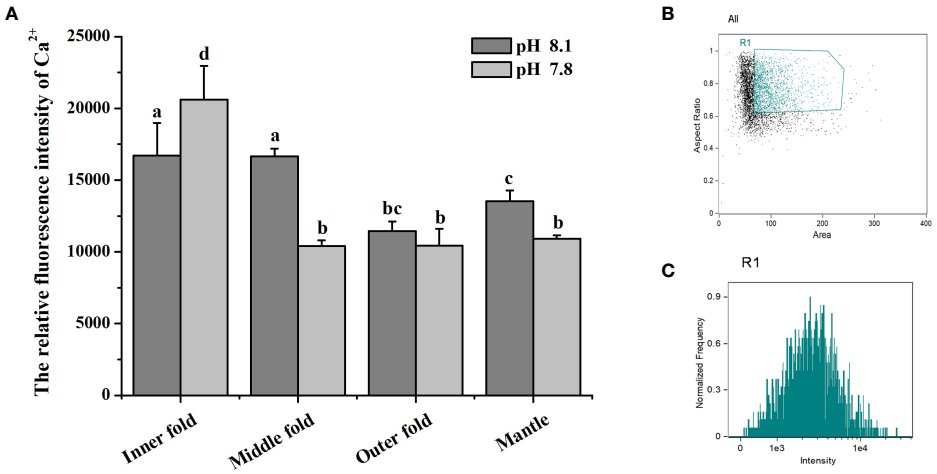

FIGURE 6
(A) Ca^{2+} content in oyster mantle cells of control group and CO_2 treatment group. Each value was shown as mean ± S.D. (N = 3), and the significant differences ($p < 0.05$) were marked by different letters (a-d). **(B, C)** Flow cytometry analysis about the fluorescence intensity of mantle cells incubated with Fluo-4 AM.

cytoplasm of *P. fucata* was able to facilitate the mRNA expression of osteopontin (Fang et al., 2008b). Mantle is the most significant tissue involved in calcification of bivalves (Bjärnmark et al., 2016; Yarra et al., 2016). In the present study, the *Cg*CaM was found to be highest expressed in mantle among all examined tissues (Figure 2), suggesting that *Cg*CaM might be involved in the calcification process of oysters. It has been reported that the numbers of EF-hand family members were higher in highly calcified species than that in low calcified species, implying that EF-hand domains were related to biomineralization (Li et al., 2016c). A EF-hand calcium-binding protein EFCBP has been demonstrated to involve in shell formation in *P. fucata* (Huang et al., 2007). *Cg*CaM was characterized as a calcium-binding protein with four EF-hand domains (Figure 1B), which was further suspected to be involved in calcification. Moreover, the epithelium of mantle is proved to be the exact region regulating the secretion and deposition of shell components (Kocot et al., 2016), and the expression and distribution of CaM in epithelium have also been reported in other bivalves (Li et al., 2004; Fang et al., 2008b). In the present study, *Cg*CaM was found to be mainly distributed in the epithelium of mantle (Figure 4). These results suggested that *Cg*CaM participated in the process of shell calcification in *C. gigas*.

Mantle is an extremely important organ in bivalves, which plays an essential role in multiple physiological processes (Brake et al., 2004; Abele et al., 2010; Itoh et al., 2010), especially calcification (Zhang et al., 2012). It is divided into three regions with respective function, which have the divergent responses to various physiological processes (Bjärnmark et al., 2016). From the umbo to posterior edge, the three regions of mantle are respectively named as central zone, submarginal zone and marginal zone, while the marginal zone can be further divided into IF, MF and OF. In the shell formation process, the distinct morphogenetic regions are responsible for the synthesis of specific shell layers. The outer periostracum is secreted by epitheliums and basal cells within the periostracal groove between the OF and the MF (Bubel, 1973; Nakayama et al., 2013). The middle prismatic layer is formed by the secretion from columnar epithelial cells in the marginal zone, while the inner nacreous layer is formed by the secretion from the submarginal zone and central zone (Fang et al., 2008a; Gardner et al., 2011; Shi et al., 2012). Most of the previous studies related to the functions of mantle in shell formation focused on the pearl oyster *P. fucata*. Many shell matrix proteins are mainly distributed in the outer mantle fold or secreted from the epithelium of the outer fold (Nakayama et al., 2013). Besides, the inner mantle fold is also related to shell calcification, it takes up ions required for calcification from the ambient medium (Marin et al., 2008). In Pacific oyster, a previous research proved that engrailed in the middle mantle fold played a major role in shell formation in response to ocean acidification (Zhang et al., 2020). In the present study, the mRNA transcripts of *Cg*CaM were found to be highly expressed in the MF among the three mantle folds of marginal zone (Figure 3), indicating that *Cg*CaM played a major role within the MF during the shell calcification. Calcification is one of the notably affected processes in bivalves in acidified environment (Chandra Rajan et al., 2021; Li et al., 2022). It was reported that the expression of calcification-related genes in mantle were significantly altered under OA to regulate the calcification process (Hüning et al., 2013; Li et al., 2016a). In the present study, the most significant change of *Cg*CaM expression occurred in the MF after acidification treatment (Figure 3). Meanwhile, the positive signal of *Cg*CaM revealed by *in situ* hybridization was found to disappear only in the outer epithelium of MF (Figure 4). The major function of the mantle MF in shell formation was proved by the previous research (Zhang et al., 2020). These results collectively suggested that *Cg*CaM in the MF of mantle played a major role in the shell calcification of *C. gigas* in response to OA.

CaM is able to bind Ca^{2+} and trigger the downstream pathways to mediate a variety of Ca^{2+}-induced physiological processes. As the most important intracellular calcium regulator (Means and Dedman, 1980; Crivici and Ikura, 1995), the no-load CaM does not possess any enzymatic or biological activity. CaM becomes active after it binds with Ca^{2+} to form Ca^{2+}-CaM complex and undergoes a conformational change to expose the hydrophobic region (Ikura, 1996; Gifford et al., 2007). When extracellular Ca^{2+} enters the cell, CaM binds Ca^{2+} more rapidly than other Ca^{2+}-binding proteins (Faas et al., 2011). In this study, *Cg*CaM was certified to display Ca^{2+}-binding activity by Ca^{2+}-dependent electrophoretic shift assay (Figure 5), implying that *Cg*CaM was able to act as an intracellular fast buffer to adjust the free Ca^{2+} levels and regulate calcium homeostasis. Ca^{2+} is the most abundant mineral as well as the primary cation in shell formation of *C. gigas*, and the regulation of calcium levels in the mantle is essential to calcification process (Rousseau et al., 2003). A series of Ca^{2+}-binding proteins, Ca^{2+}-exchangers, Ca^{2+}-channels and Ca^{2+}-ATPases in mantle have been demonstrated to participate in Ca^{2+} absorption, transport and deposition in order to maintain the calcium homeostasis (Sillanpää et al., 2018; Sillanpää et al., 2020). The expression of these above genes changed greatly under OA stress, which resulted in the calcium homeostasis disequilibrium in marine bivalves (Wang et al., 2020). In the present study, the expression level of *Cg*CaM in the MF of mantle decreased significantly (Figure 3), and the content of Ca^{2+} was also significantly reduced after *C. gigas* was exposed to the acidified seawater (Figure 6). Similarly, the significant change of CaM and CaLP expression under long-term OA treatment was also reported to alter the free Ca^{2+} concentration in mantle cells of *P. fucata* (Li et al., 2016a). These results inferred that the down-regulated expression of *Cg*CaM under OA resulted in the alteration of Ca^{2+} content in the mantle MF, which might inhibit calcification process of *C. gigas*.

In summary, a *Cg*CaM with four continuous EF-hand domains was characterized to exhibit Ca^{2+}-binding activity in oyster *C. gigas*. The highest mRNA expression level of *Cg*CaM was detected in the MF of mantle. The mRNA expression of

*Cg*CaM and Ca^{2+} content in the MF of mantle decreased significantly after the acidification treatment. These results suggested that *Cg*CaM might affect the calcification process of *C. gigas* under OA by regulating calcium homeostasis in the MF of mantle.

Data availability statement

The original contributions presented in the study are included in the article/supplementary material. Further inquiries can be directed to the corresponding authors.

Author contributions

XX, CL, and ZL conceived and designed the experiments. XX, YZ, YG, and TZ performed the experiments. XX and CL analyzed the data. ZL, LW, and LS contributed reagents, materials, and analysis tools. XX wrote the original manuscript. CL, LW and LS revised and approved the manuscript. All authors contributed to the article and approved the submitted version.

Funding

We are grateful to all the laboratory members for their technical advice and helpful discussions. This research was supported by NSFC grants (Nos. 32072946), National Key R&D Program (2018YFD0900606), the earmarked fund for CARS-49, the Fund for Outstanding Talents and Innovative Team of Agricultural Scientific Research, the Distinguished Professor of Liaoning (XLYC1902012), and Talented Scholars in Dalian Ocean University.

Acknowledgments

We are grateful to all the laboratory members for their technical advice and helpful discussions.

Conflict of interest

The authors declare that the research was conducted in the absence of any commercial or financial relationships that could be construed as a potential conflict of interest.

Publisher's note

All claims expressed in this article are solely those of the authors and do not necessarily represent those of their affiliated organizations, or those of the publisher, the editors and the reviewers. Any product that may be evaluated in this article, or claim that may be made by its manufacturer, is not guaranteed or endorsed by the publisher.

References

Abele, D., Kruppe, M., Philipp, E. E., and Brey, T. (2010). Mantle cavity water oxygen partial pressure (PO_2) in marine molluscs aligns with lifestyle. *Can. J. Fish. Aquat. Sci.* 67 (6), 977–986. doi: 10.1139/F10-035

Addadi, L., Joester, D., Nudelman, F., and Weiner, S. (2006). Mollusk shell formation: A source of new concepts for understanding biomineralization processes. *Chemistry* 12 (4), 980–987. doi: 10.1002/chem.200500980

Audino, J. A., Marian, J. E., Wanninger, A., and Lopes, S. G. (2015). Mantle margin morphogenesis in *Nodipecten nodosus* (Mollusca: Bivalvia): New insights into the development and the roles of bivalve pallial folds. *BMC Dev. Biol.* 15, 22. doi: 10.1186/s12861-015-0074-9

Babu, Y. S., Bugg, C. E., and Cook, W. J. (1988). Structure of calmodulin refined at 2.2 a resolution. *J. Mol. Biol.* 204 (1), 191–204. doi: 10.1016/0022-2836(88)90608-0

Bednaršek, N., Feely, R. A., Reum, J. C., Peterson, B., Menkel, J., Alin, S. R., et al. (2014). *Limacina helicina* shell dissolution as an indicator of declining habitat suitability owing to ocean acidification in the California current ecosystem. *Proc. Biol. Sci.* 281 (1785), 20140123. doi: 10.1098/rspb.2014.0123

Bjärnmark, N. A., Yarra, T., Churcher, A. M., Felix, R. C., Clark, M. S., and Power, D. M. (2016). Transcriptomics provides insight into *Mytilus galloprovincialis* (Mollusca: Bivalvia) mantle function and its role in biomineralisation. *Mar. Genom.* 27, 37–45. doi: 10.1016/j.margen.2016.03.004

Brake, J., Evans, F., and Langdon, C. (2004). Evidence for genetic control of pigmentation of shell and mantle edge in selected families of pacific oysters, *Crassostrea gigas*. *Aquaculture* 229 (1-4), 89–98. doi: 10.1016/S0044-8486(03)00325-9

Bubel, A. (1973). An electron-microscope study of periostracum formation in some marine bivalves. II. The cells lining the periostracal groove. *Mar. Biol.* 20 (3), 222–234. doi: 10.1007/BF00348988

Burgess, W. H., Jemiolo, D. K., and Kretsinger, R. H. (1980). Interaction of calcium and calmodulin in the presence of sodium dodecyl sulfate. *Biochim. Biophys. Acta* 623 (2), 257–270. doi: 10.1016/0005-2795(80)90254-8

Caldeira, K., and Wickett, M. E. (2003). Oceanography: Anthropogenic carbon and ocean pH. *Nature* 425 (6956), 365. doi: 10.1038/425365a

Chandra Rajan, K., Meng, Y., Yu, Z., Roberts, S. B., and Vengatesen, T. (2021). Oyster biomineralization under ocean acidification: From genes to shell. *Glob. Change Biol.* 27 (16), 3779–3797. doi: 10.1111/gcb.15675

Chandra Rajan, K., and Vengatesen, T. (2020). Molecular adaptation of molluscan biomineralisation to high-CO_2 oceans - the known and the unknown. *Mar. Environ. Res.* 155, 104883. doi: 10.1016/j.marenvres.2020.104883

Cheung, W. Y. (1984). Calmodulin: Its potential role in cell proliferation and heavy metal toxicity. *Fed. Proc.* 43 (15), 2995–2999.

Clapham, D. E. (2007). Calcium signaling. *Cell* 131 (6), 1047–1058. doi: 10.1016/j.cell.2007.11.028

Crivici, A., and Ikura, M. (1995). Molecular and structural basis of target recognition by calmodulin. *Annu. Rev. Biophys. Biomol. Struct.* 24, 85–116. doi: 10.1146/annurev.bb.24.060195.000505

Doney, S. C., Fabry, V. J., Feely, R. A., and Kleypas, J. A. (2009). Ocean acidification: The other CO_2 problem. *Ann. Rev. Mar. Sci.* 1, 169–192. doi: 10.1146/annurev.marine.010908.163834

Faas, G. C., Raghavachari, S., Lisman, J. E., and Mody, I. (2011). Calmodulin as a direct detector of Ca^{2+} signals. *Nat. Neurosci.* 14 (3), 301–304. doi: 10.1038/nn.2746

Fang, Z., Feng, Q., Chi, Y., Xie, L., and Zhang, R. (2008a). Investigation of cell proliferation and differentiation in the mantle of *Pinctada fucata* (Bivalve, Mollusca). *Mar. Biol.* 153 (4), 745–754. doi: 10.1007/s00227-007-0851-5

Fang, Z., Yan, Z., Li, S., Wang, Q., Cao, W., Xu, G., et al. (2008bb). Localization of calmodulin and calmodulin-like protein and their functions in biomineralization in *P. fucata*. *Prog. Nat. Sci.* 18 (4), 405–412. doi: 10.1016/j.pnsc.2007.11.011

Feely, R. A., Sabine, C. L., Lee, K., Berelson, W., Kleypas, J., Fabry, V. J., et al. (2004). Impact of anthropogenic CO_2 on the $CaCO_3$ system in the oceans. *Science* 305 (5682), 362–366. doi: 10.1126/science.1097329

Field, C. B., and Barros, V. R. (2014). *Climate change 2014: impacts, adaptation, and vulnerability. part a: global and sectoral aspects* (Cambridge: University Press).

Föller, M., Bobbala, D., Koka, S., Boini, K. M., Mahmud, H., Kasinathan, R. S., et al. (2010). Functional significance of the intermediate conductance Ca^{2+}-activated k^+ channel for the short-term survival of injured erythrocytes. *Pflugers Arch.* 460 (6), 1029–1044. doi: 10.1007/s00424-010-0878-1

Gardner, L. D., Mills, D., Wiegand, A., Leavesley, D., and Elizur, A. (2011). Spatial analysis of biomineralization associated gene expression from the mantle organ of the pearl oyster *Pinctada maxima*. *BMC Genomics* 12, 455. doi: 10.1186/1471-2164-12-455

Gifford, J. L., Walsh, M. P., and Vogel, H. J. (2007). Structures and metal-ion-binding properties of the Ca^{2+}-binding helix-loop-helix EF-hand motifs. *Biochem. J.* 405 (2), 199–221. doi: 10.1042/BJ20070255

Hendriks, I. E., Duarte, C. M., Olsen, Y. S., Steckbauer, A., Ramajo, L., Moore, T. S., et al. (2015). Biological mechanisms supporting adaptation to ocean acidification in coastal ecosystems. *Estuar. Coast. Shelf Sci.* 152, A1–A8. doi: 10.1016/j.ecss.2014.07.019

Hettinger, A., Sanford, E., Hill, T., Hosfelt, J., Russell, A., and Gaylord, B. (2013). The influence of food supply on the response of Olympia oyster larvae to ocean acidification. *Biogeosciences* 10 (10), 6629–6638. doi: 10.5194/bgd-10-5781-2013

Huang, W., Yao, B., Sun, L., Pu, R., Wang, L., and Zhang, R. (2001). Immunohistochemical and *in situ* hybridization studies of gonadotropin releasing hormone (GnRH) and its receptor in rat digestive tract. *Life Sci.* 68 (15), 1727–1734. doi: 10.1016/s0024-3205(01)00968-7

Huang, J., Zhang, C., Ma, Z., Xie, L., and Zhang, R. (2007). A novel extracellular EF-hand protein involved in the shell formation of pearl oyster. *Biochim. Biophys. Acta* 1770 (7), 1037–1044. doi: 10.1016/j.bbagen.2007.03.006

Hüning, A. K., Melzner, F., Thomsen, J., Gutowska, M. A., Krämer, L., Frickenhaus, S., et al. (2013). Impacts of seawater acidification on mantle gene expression patterns of the Baltic Sea blue mussel: Implications for shell formation and energy metabolism. *Mar. Biol.* 160 (8), 1845–1861. doi: 10.1007/s00227-012-1930-9

Ikura, M. (1996). Calcium binding and conformational response in EF-hand proteins. *Trends Biochem. Sci.* 21 (1), 14–17. doi: 10.1016/S0968-0004(06)80021-6

Itoh, N., Okada, Y., Takahashi, K. G., and Osada, M. (2010). Presence and characterization of multiple mantle lysozymes in the pacific oyster, *Crassostrea gigas*. *Fish Shellfish Immunol.* 29 (1), 126–135. doi: 10.1016/j.fsi.2010.02.027

Johnson, K. L., Zhen, D. K., and Bianchi, D. W. (2000). The use of fluorescence *in situ* hybridization (FISH) on paraffin-embedded tissue sections for the study of microchimerism. *Biotechniques* 29 (6), 1220–1224. doi: 10.2144/00296st01

Kádár, E. (2008). Haemocyte response associated with induction of shell regeneration in the deep-sea vent mussel *Bathymodiolus azoricus* (Bivalvia: Mytilidae). *J. Exp. Mar. Biol. Ecol.* 362 (2), 71–78. doi: 10.1016/j.jembe.2008.05.014

Kocot, K. M., Aguilera, F., McDougall, C., Jackson, D. J., and Degnan, B. M. (2016). Sea Shell diversity and rapidly evolving secretomes: Insights into the evolution of biomineralization. *Front. Zool.* 13, 23. doi: 10.1186/s12983-016-0155-z

Kretsinger, R. H. (1997). EF-hands embrace. *Nat. Struct. Biol.* 4 (7), 514–516. doi: 10.1038/nsb0797-514

Li, S., Huang, J., Liu, C., Liu, Y., Zheng, G., Xie, L., et al. (2016a). Interactive effects of seawater acidification and elevated temperature on the transcriptome and biomineralization in the pearl oyster *Pinctada fucata*. *Environ. Sci. Technol.* 50 (3), 1157–1165. doi: 10.1021/acs.est.5b05107

Li, S., Liu, C., Huang, J., Liu, Y., Zhang, S., Zheng, G., et al. (2016b). Transcriptome and biomineralization responses of the pearl oyster *Pinctada fucata* to elevated CO_2 and temperature. *Sci. Rep.* 6, 18943. doi: 10.1038/srep18943

Livak, K. J., and Schmittgen, T. D. (2001). Analysis of relative gene expression data using real-time quantitative PCR and the $2^{-\Delta\Delta CT}$ method. *Methods* 25 (4), 402–408. doi: 10.1006/meth.2001.1262

Li, S., Xie, L., Zhang, C., Zhang, Y., Gu, M., and Zhang, R. (2004). Cloning and expression of a pivotal calcium metabolism regulator: Calmodulin involved in shell formation from pearl oyster (*Pinctada fucata*). *Comp. Biochem. Physiol. B Biochem. Mol. Biol.* 138 (3), 235–243. doi: 10.1016/j.cbpc.2004.03.012

Li, X., Yu, W., Cai, Z., He, C., Wei, N., Wang, X., et al. (2016c). Molecular cloning and characterization of full-length cDNA of calmodulin gene from pacific oyster *Crassostrea gigas*. *Biomed. Res. Int.* 2016, 5986519. doi: 10.1155/2016/5986519

Li, J., Zhou, Y., Qin, Y., Wei, J., Shigong, P., Ma, H., et al. (2022). Assessment of the juvenile vulnerability of symbiont-bearing giant clams to ocean acidification. *Sci. Total Environ.* 812, 152265. doi: 10.1016/j.scitotenv.2021.152265

Lv, X., Wang, W., Han, Z., Liu, S., Yang, W., Li, M., et al. (2019). The dicer from oyster *Crassostrea gigas* functions as an intracellular recognition molecule and effector in anti-viral immunity. *Fish Shellfish Immunol.* 95, 584–594. doi: 10.1016/j.fsi.2019.10.067

Marin, F., Le Roy, N., and Marie, B. (2012). The formation and mineralization of mollusk shell. *Front. Biosci. (Schol. Ed.)* 4 (3), 1099–1125. doi: 10.2741/s321

Marin, F., Luquet, G., Marie, B., and Medakovic, D. (2008). Molluscan shell proteins: primary structure, origin, and evolution. *Curr. Top. Dev. Biol.* 80, 209–276. doi: 10.1016/S0070-2153(07)80006-8

Means, A. R., and Dedman, J. R. (1980). Calmodulin–an intracellular calcium receptor. *Nature* 285 (5760), 73–77. doi: 10.1038/285073a0

Mount, A. S., Wheeler, A. P., Paradkar, R. P., and Snider, D. (2004). Hemocyte-mediated shell mineralization in the eastern oyster. *Science* 304 (5668), 297–300. doi: 10.1126/science.1090506

Nakayama, S., Suzuki, M., Endo, H., Iimura, K., Kinoshita, S., Watabe, S., et al. (2013). Identification and characterization of a matrix protein (PPP-10) in the periostracum of the pearl oyster, *Pinctada fucata*. *FEBS Open Bio* 3, 421–427. doi: 10.1016/j.fob.2013.10.001

Orr, J. C., Fabry, V. J., Aumont, O., Bopp, L., Doney, S. C., Feely, R. A., et al. (2005). Anthropogenic ocean acidification over the twenty-first century and its impact on calcifying organisms. *Nature* 437 (7059), 681–686. doi: 10.1038/nature04095

Peng, K., Liu, F. L., Wang, J. H., and Hong, Y. J. (2018). Calmodulin highly expressed during the formation of pearl sac in freshwater pearl mussel (*Hyriopsis schlegelii*). *Thalassas: an Int. J. Mar. Sci.* 34 (1), 219–225. doi: 10.1007/s41208-017-0054-x

Richards, M., Xu, W., Mallozzi, A., Errera, R. M., and Supan, J. (2018). Production of calcium-binding proteins in *Crassostrea virginica* in response to increased environmental CO_2 concentration. *Front. Mar. Sci.* 5. doi: 10.3389/fmars.2018.00203

Ross, P. M., Parker, L., O'Connor, W. A., and Bailey, E. A. (2011). The impact of ocean acidification on reproduction, early development and settlement of marine organisms. *Water* 3 (4), 1005–1030. doi: 10.3390/w3041005

Rousseau, M., Plouguerne, E., Wan, G., Wan, R., Lopez, E., and Fouchereau-Peron, M. (2003). Biomineralisation markers during a phase of active growth in *Pinctada margaritifera*. *Comp. Biochem. Physiol. A Mol. Integr. Physiol.* 135 (2), 271–278. doi: 10.1016/s1095-6433(03)00070-9

Schwaller, B. (2012). The regulation of a cell's Ca^{2+} signaling toolkit: the Ca^{2+} homeostasome. *Adv. Exp. Med. Biol.* 740, 1–25. doi: 10.1007/978-94-007-2888-2_1

Sée, V., Boutillier, A. L., Bito, H., and Loeffler, J. P. (2001). Calcium/calmodulin-dependent protein kinase type IV (CaMKIV) inhibits apoptosis induced by potassium deprivation in cerebellar granule neurons. *FASEB J.* 15 (1), 134–144. doi: 10.1096/fj.00-0106com

Senawong, G., Laha, T., Loukas, A., Brindley, P. J., and Sripa, B. (2012). Cloning, expression, and characterization of a novel *Opisthorchis viverrini* calcium-binding EF-hand protein. *Parasitol. Int.* 61 (1), 94–100. doi: 10.1016/j.parint.2011.07.012

Shi, S., Jiao, Y., Du, X., and Zhang, Y. (2012). Ultrastructure of mantle epithelial cells in *Pinctada martensii*. *Guangdong Agric. Sci.* 39, 135–137.

Sillanpää, J. K., Cardoso, J., Félix, R. C., Anjos, L., Power, D. M., and Sundell, K. (2020). Dilution of seawater affects the Ca^{2+} transport in the outer mantle epithelium of *Crassostrea gigas*. *Front. Physiol.* 11. doi: 10.3389/fphys.2020.00001

Sillanpää, J. K., Sundh, H., and Sundell, K. S. (2018). Calcium transfer across the outer mantle epithelium in the pacific oyster, *Crassostrea gigas*. *Proc. Biol. Sci.* 285, 20181676. doi: 10.1098/rspb.2018.1676

Simkiss, K., and Wilbur, K. M. (1989). Biomineralization, Harcourt Brace Jovanovich. (Academic Press)

Stevens, F. C. (1983). Calmodulin: an introduction. *Can. J. Biochem. Cell Biol.* 61 (8), 906–910. doi: 10.1139/o83-115

Thomsen, J., Haynert, K., Wegner, K. M., and Melzner, F. (2015). Impact of seawater carbonate chemistry on the calcification of marine bivalves. *Biogeosciences* 12 (14), 4209–4220. doi: 10.5194/bg-12-4209-2015

Waldbusser, G. G., Brunner, E. L., Haley, B. A., Hales, B., Langdon, C. J., and Prahl, F. G. (2013). A developmental and energetic basis linking larval oyster shell formation to acidification sensitivity. *Geophys. Res. Lett.* 40 (10), 2171–2176. doi: 10.1002/grl.50449

Wang, X., Li, C., Lv, Z., Zhang, Z., and Qiu, L. (2022). A calcification-related calmodulin-like protein in the oyster *Crassostrea gigas* mediates the enhanced calcium deposition induced by CO_2 exposure. *Sci. Total Environ.* 833, 155114. doi: 10.1016/j.scitotenv.2022.155114

Wang, X., Wang, M., Wang, W., Liu, Z., Xu, J., Jia, Z., et al. (2020). Transcriptional changes of pacific oyster *Crassostrea gigas* reveal essential role of calcium signal pathway in response to CO_2-driven acidification. *Sci. Total Environ.* 741, 140177. doi: 10.1016/j.scitotenv.2020.140177

Yan, Z., Fang, Z., Ma, Z., Deng, J., Li, S., Xie, L., et al. (2007). Biomineralization: functions of calmodulin-like protein in the shell formation of pearl oyster. *Biochim. Biophys. Acta* 1770 (9), 1338–1344. doi: 10.1016/j.bbagen.2007.06.018

Yarra, T., Gharbi, K., Blaxter, M., Peck, L. S., and Clark, M. S. (2016). Characterization of the mantle transcriptome in bivalves: *Pecten maximus*, *Mytilus edulis* and *Crassostrea gigas*. *Mar. Genom* 27, 9–15. doi: 10.1016/j.margen.2016.04.003

Zhang, G., Fang, X., Guo, X., Li, L., Luo, R., Xu, F., et al. (2012). The oyster genome reveals stress adaptation and complexity of shell formation. *Nature* 490, 49–54. doi: 10.1038/nature11413

Zhang, Y., Liu, Z., Song, X., Huang, S., Wang, L., and Song, L. (2019). The inhibition of ocean acidification on the formation of oyster calcified shell by regulating the expression of *Cg*chs1 and *Cg*chit4. *Front. Physiol.* 10, 1034. doi: 10.3389/fphys.2019.01034

Zhang, Y., Liu, Z., Zong, Y., Zheng, Y., Li, Y., Han, Z., et al. (2020). The increased expression of an engrailed to sustain shell formation in response to ocean acidification. *Front. Physiol.* 11. doi: 10.3389/fphys.2020.530435

Zhou, Y., Xue, S., and Yang, J. J. (2013). Calciomics: integrative studies of Ca^{2+}-binding proteins and their interactomes in biological systems. *Metallomics* 5 (1), 29–42. doi: 10.1039/c2mt20009k

Zoccola, D., Tambutte, E., Kulhanek, E., Puverel, S., Scimeca, J. C., Allemand, D., et al. (2004). Molecular cloning and localization of a PMCA p-type calcium ATPase from the coral *Stylophora pistillata*. *Biochim. Biophys. Acta* 1663 (1-2), 117–126. doi: 10.1016/j.bbamem.2004.02.010